

# Precoder-Aided Iterative Detection Assisted Multilevel Coding and Three-Dimensional EXIT-Chart Analysis

R. Y. S. Tee, S. X. Ng and <sup>1</sup>L. Hanzo

School of ECS, University of Southampton, SO17 1BJ, UK.  
 Tel: +44-23-8059 3125, Fax: +44-23-8059 4508  
 Email: <sup>1</sup>lh@ecs.soton.ac.uk, http://www-mobile.ecs.soton.ac.uk

**Abstract** – A novel three-dimensional (3D) EXIT chart is developed for investigating the iterative behaviour of Multilevel Coding (MLC) invoking Multistage Decoding (MSD). The extrinsic information transfer characteristics of both the symbol-to-bit demapper used and those of the different-protection constituent decoders suggest that potential improvements can be achieved by appropriately designing the demapper. The proposed 3D EXIT chart is then invoked for studying the precoder-aided multilevel coding scheme employing both MSD and Parallel Independent Decoding (PID) for communicating over AWGN and uncorrelated Rayleigh fading channels with the aid of 8PSK modulation. At BER= $10^{-5}$ , the precoder was capable of enhancing the achievable  $E_b/N_0$  performance by 0.5dB to 2.5dB over AWGN and Rayleigh channels, respectively.

performance with the aid of optimized bit-to-symbol mappers / demappers [2] [4] [5]. In this paper, instead of optimizing the modem constellation labelling, we introduce a serially concatenated unity-rate code [6] having a recursive structure as a precoder in the context of MLC schemes for the sake of enhancing the demapper’s convergence characteristics. Furthermore, we will benchmark our MLC MSD scheme against the Parallel Independent Decoding (PID) [2] scheme, which exhibits a significantly reduced decoding delay.

The rest of this contribution is organized as follows. Section 2 provides an overview of the system considered, while our novel 3D EXIT chart is invoked in Section 3 for the sake of characterizing the system’s iterative convergence behaviour. Section 4 quantifies the performance of our pre-coded MLC scheme, while our conclusions are presented in Section 5.

## 1. INTRODUCTION

Multilevel Coding (MLC) was introduced by Imai and Hirawaki [1] as a bandwidth efficient coded modulation scheme, which was designed for protecting each bit of non-binary modulation schemes with the aid of potentially different-rate binary codes. The so-called capacity rules have been proposed [2] for choosing appropriate coding rates that are capable of approaching the channel capacity with the aid of Multistage Decoding (MSD), while Parallel Independent Decoding (PID) has been employed as a design alternative for the sake of reducing the associated decoding delay. However, the iterative decoding behaviour of MLC schemes depends on the mutual information transfer characteristics of both the decoders as well as on those of the demapper used for conveying the demodulated bits to the constituent decoders.

With the objective of studying the iterative detection aided performance of MSD assisted MLCs, we propose a novel three-dimensional (3D) extrinsic information transfer (EXIT) [3] chart for investigating the effects of different symbol-to-bit demapper characteristics. In the recent past, different constellation labeling strategies have been employed in the context of MLC for the sake of increasing either the Euclidean distance or the Hamming distance associated with the different modulation phasor points in order to achieve a better iterative detection

The financial support of the European Union under the auspices of the Phoenix and Newcom projects and that of the EPSRC, UK is gratefully acknowledged.

## 2. SYSTEM OVERVIEW

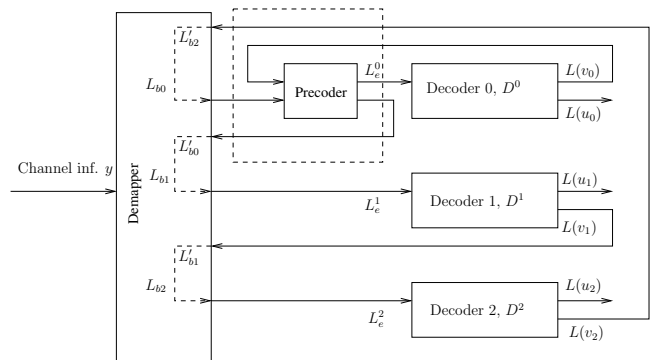


Figure 1: MSD Decoder of the 8PSK modulation based precoder-aided MLC scheme.

Figure 1 and 2 outline our MSD and PID schemes designed for operating in conjunction with 8PSK modulation, respectively. The notations  $L(u_i)$  and  $L(v_i)$  represent the output LLRs of the decoders for the original information bits and for the MLC-encoded bits, respectively. The subscript  $i$  represents the index of the different-protection bits  $b_0$ ,  $b_1$  and  $b_2$ , while  $L_e^i$  denotes the *extrinsic* LLR generated at the output of the *inner* demapper. The rectangle drawn in dashed lines in both Figures 1 and 2 represents the precoder schemes constituted by unity-rate recursive encoders inserted after the demapper. In Figure 1,  $L_{bi}$  denotes the associated information bits’ LLRs for

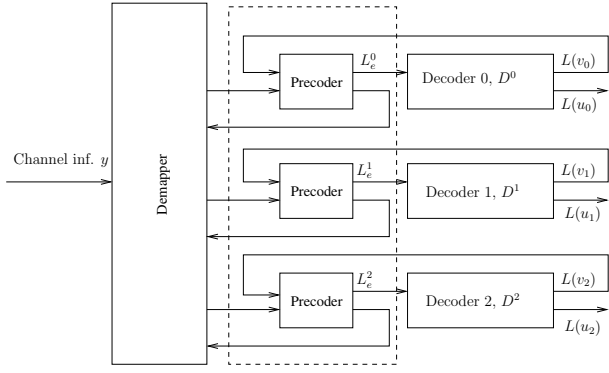


Figure 2: PID Decoder of the 8PSK modulation based precoder-aided MLC scheme.

the corresponding decoder  $D^i$ , while  $L'_{bi}$  denotes the *a priori* LLRs forwarded by the *other* decoder  $D^i$  to the input of the inner demapper.

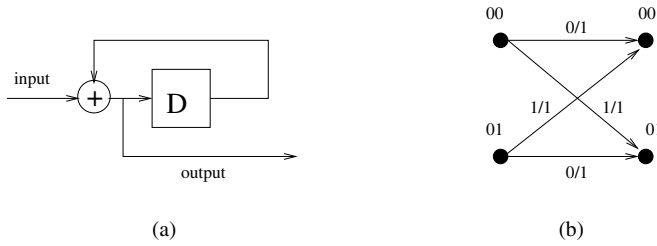


Figure 3: Unity rate memory-1 precoder

To elaborate a little further, in the MSD decoder of Figure 1 the *a priori* information is fed by the lower-protection decoder to the higher-protection scheme. Each of the bits  $b_0$ ,  $b_1$  and  $b_2$  is decoded by the corresponding decoder, namely by  $D^0$ ,  $D^1$  and  $D^2$ . The decoder  $D^i$  processes both the received information bits of  $L_{bi}$  as well as the *a priori* information provided by the *other* decoders and conveyed by the inner demapper seen in Figure 1. By contrast, the PID structure shown in Figure 2 does not make use of the decisions carried out at other protection levels. Instead, each decoder  $D^i$  processes the *a priori* knowledge in a parallel and independent manner. Hence, this potentially results in a reduction of the associated processing delay.

Figure 3 portrays the unity-rate code employed in our precoder-aided MLC scheme, where  $D$  is a shift register stage and  $\oplus$  represents the modulo-2 operation. Figure 3(b) shows the trellis diagram of the precoder. The trellis transitions are denoted by  $c_i/x_i$ , where  $c_i$  denotes the input of the precoder at time  $i$ , while  $x_i$  indicates the corresponding precoder output.

In the system advocated, we employ convolutional codes as our component, where the individual coding rates of the MLC MSD and MLC PID schemes are 1/3, 3/4, 11/12 [7] and 1/2, 3/4 and 3/4 [2], respectively. Since the specific coding rates that are readily available for convolutional codes are constrained, we do not follow the exact capacity rules proposed in [2] for adjusting the MLC scheme's coding rate. The resultant effective throughput of the 8PSK system considered becomes

2 bits per symbol. All system parameters are summarized in Table 1.

Coding rate	$R_0$	$R_1$	$R_2$
MSD	1/3	3/4	11/12
PID	1/2	3/4	3/4
Precoders' trellis states	00 and 01		
Modulation	8PSK		
Mapping type	Set Partitioning (SP)		
Interleaver length	1800 symbols		

Table 1: System parameters.

### 3. EXIT CHART BASED CONVERGENCE ANALYSIS

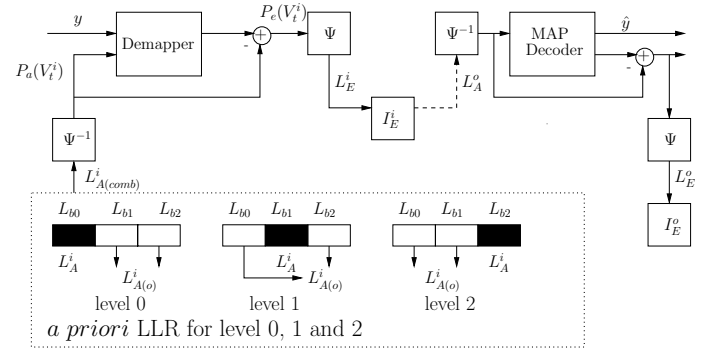


Figure 4: EXIT chart generation for the MSD of 3-level MLC when using 8PSK and three en(de)coders.

In this section, we introduce a 3D EXIT chart for the sake of analyzing the iterative convergence behaviour of the MLC MSD scheme considered, where the demapper and decoder are referred to as the *inner* and *outer* codes. Figure 4 shows the schematic of generating the 3D EXIT chart. Specifically,  $L_b^a$  represents the LLR values, where the superscript  $a$  denotes the inner ( $i$ ) or outer ( $o$ ) codes, while the subscript  $b$  denotes the input *a priori* ( $A$ ) or output *extrinsic* ( $E$ ) information. The variables  $L_{b0}$ ,  $L_{b1}$  and  $L_{b2}$  are independent Gaussian distributed LLRs generated for bits 0, 1 and 2, respectively. Furthermore,  $\Psi$  and  $\Psi^{-1}$  denote the LLR-to-symbol probability and symbol probability-to-LLR conversion. The arrow drawn in dashed line represents the *extrinsic* LLR demapper output, which becomes the LLR input of the decoder after demapping. The filled black box represents the *a priori* LLR of the associated information bit, while the hollow box denotes the *a priori* LLR of the *other* decoders' bits. Both  $I_E^i$  and  $I_E^o$ , which denote the mutual information accruing from the *inner* and *outer* codes are used for plotting the EXIT chart.

In order to generate the 3D EXIT chart for the MLC MSD scheme seen in Figure 1 for an 8PSK modulated system, we model the LLRs  $L_A^i$  and  $L_{A(o)}^i$  by independent Gaussian distributed random variables [3] at MLC protection level 0, 1 and 2, as shown in Figure 4. Considering the example of protection *level* 0, the LLR  $L_A^i$  associated with the black box in Figure 4 is generated from  $L_{b0}$ . The *a priori* LLRs  $L_{b1}$  and  $L_{b2}$  gener-



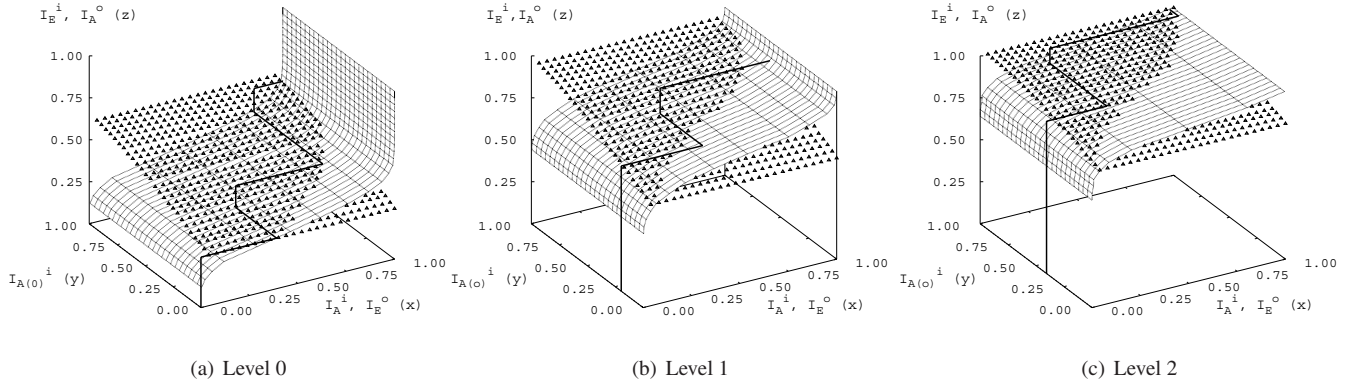


Figure 5: 3D EXIT Chart for Level 0, Level 1 and Level 2 of the MLC scheme at SNR = 4dB.

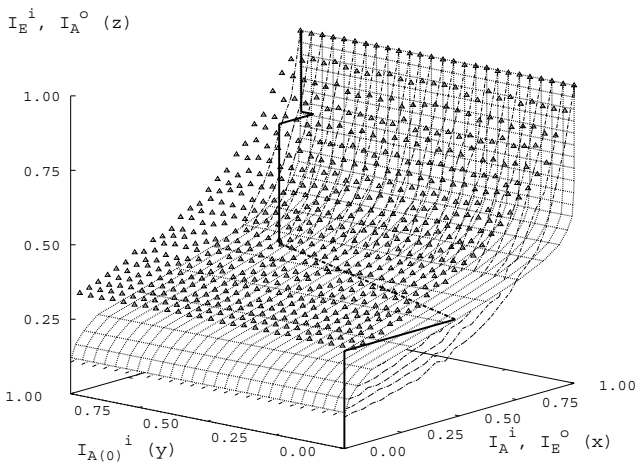


Figure 7: 3D EXIT chart for protection level 0 of the precoder-aided MLC scheme of Figure 1 at SNR = 4dB (dotted dashed lines) and SNR = 6dB (mesh of triangles).

Figures 10 and 11 illustrate the attainable BER performance of the precoder-aided MLC PID scheme communicating over both AWGN and uncorrelated Rayleigh fading channels. At BER=10<sup>-5</sup>, the precoder-aided MLC scheme exhibits a significant coding advantage of about 2dB in AWGN channels and about 5dB in uncorrelated Rayleigh channels. Note that PID becomes capable of outperforming MSD in the precoder-aided MLC scheme, as the benefit of its higher iteration gain. This is due to the fact that the decision errors of the lower protection levels may spread to the higher levels in MSD. Furthermore, SP-based mapping, which maximizes the Euclidean distance of phasor constellation points for the sake of obtaining an iteration gain, performs better in AWGN channels. In Figure 12, we further compare the precoder-aided MLC PID scheme to other coded modulation schemes having the same expressed complexity in terms of the number of trellis states

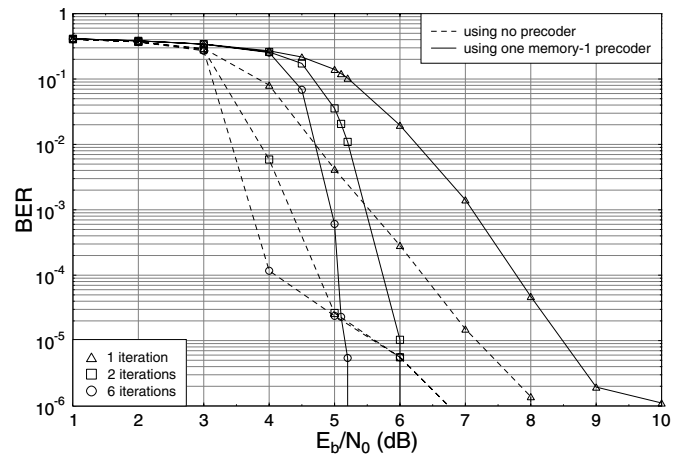


Figure 8: BER versus  $E_b/N_0$  performance of the conventional and precoder-aided 8PSK modulated MLC MSD scheme of Figure 1, communicating over an AWGN channel.

and communicating over uncorrelated Rayleigh fading channels. Our precoder-aided MLC scheme exhibits a better BER performance associated with a coding advantage of 2.5dB at BER=10<sup>-5</sup> compared to the best-performing BICM-ID coded modulation scheme, although it is outperformed by TCM, both of which were detailed in [9].

## 5. CONCLUSIONS

In conclusion, this paper provides an insight into the iterative decoding convergence behaviour of precoder-aided MLC MSD and MLC PID schemes. We proposed the novel tool of 3D EXIT charts for the sake of investigating the iterative convergence of precoder-aided MLC schemes. Our simulation results outlined in Figures 8, 9, 10 and 11 illustrate that the precoder-aided iterative MLC scheme achieves a significant BER performance improvement both in AWGN and uncorrelated Rayleigh channels, which is achieved without reducing the overall coding rate and without significantly increasing the complexity of the conventional MLC scheme. Alter-

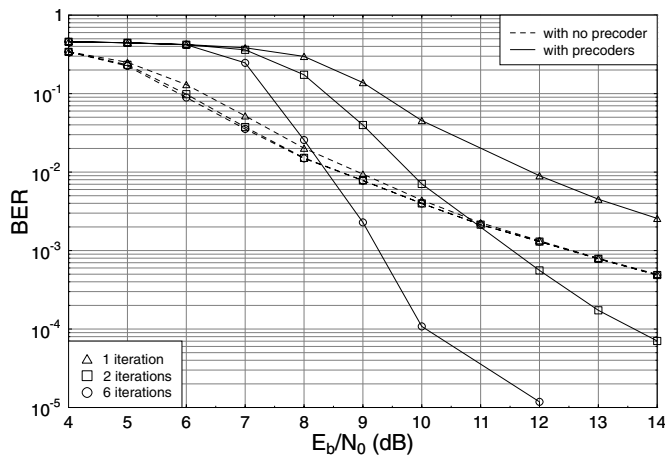


Figure 9: BER versus  $E_b/N_0$  performance of both conventional and precoder-aided 8PSK modulated MLC MSD scheme, communicating over uncorrelated Rayleigh channel.

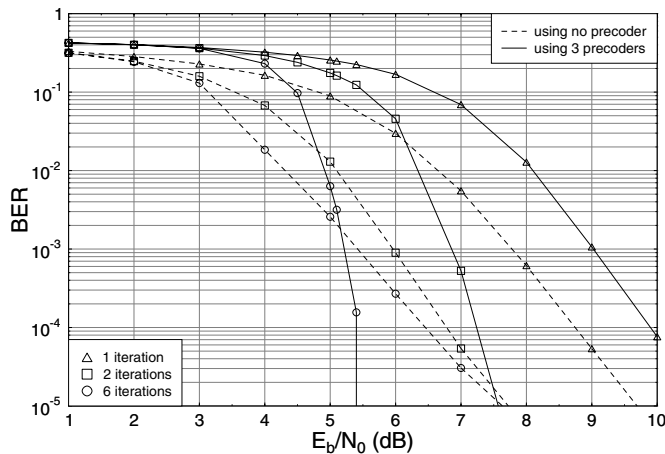


Figure 10: BER versus  $E_b/N_0$  performance of both conventional and precoder-aided 8PSK modulated MLC PID scheme, communicating over AWGN channel.

natively, at  $\text{BER}=10^{-5}$  the precoder was capable of enhancing the achievable  $E_b/N_0$  performance by 0.5dB and 5dB, when communicating over AWGN and Rayleigh channels, respectively. Our future research investigates the iterative decoding performance of combined MLCs and Generalized Low-Density Parity-Check (GLDPC) codes.

## 6. REFERENCES

- [1] H. Imai and S. Hirawaki, "A New Multilevel Coding Method Using Error Correcting Codes," *IEEE Transactions on Information Theory*, pp. 371–377, May 1977.
- [2] U. Wachsmann, R. F. H. Fischer and J. B. Huber, "Multilevel Codes: Theoretical Concepts and Practical Design Rules," *IEEE Transaction on Information Theory*, vol. 45, pp. 1361–1391, July 1999.
- [3] S. ten Brink, "Convergence Behavior of Iteratively Decoded Parallel Concatenated Codes," *IEEE Transactions On Communications*, pp. 1727–1737, October 2001.

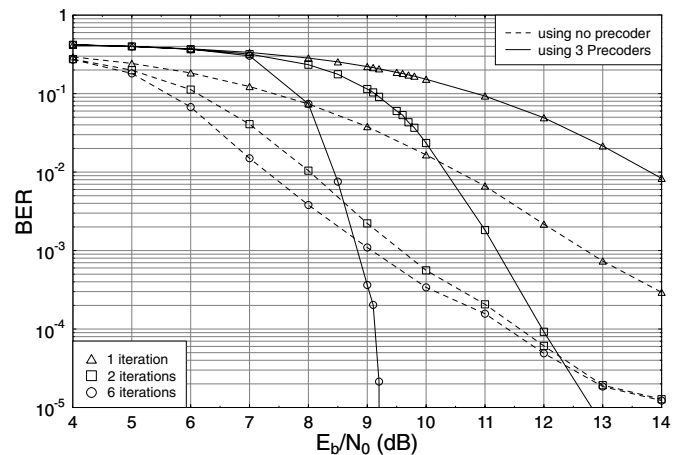


Figure 11: BER versus  $E_b/N_0$  performance of both conventional and precoder-aided 8PSK modulated MLC PID schemes, communicating over uncorrelated Rayleigh channels.

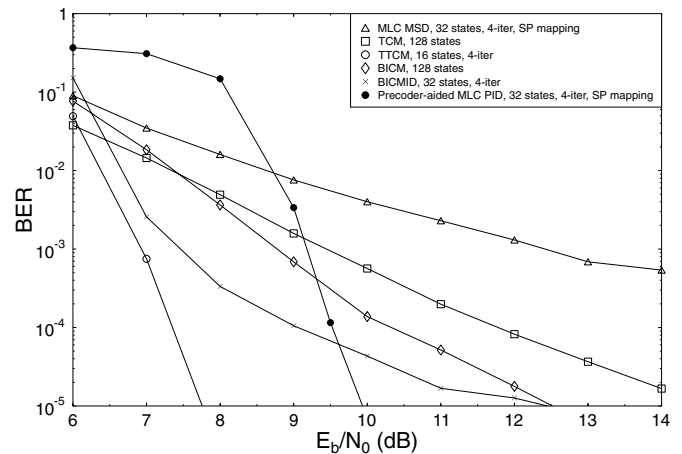


Figure 12: BER versus  $E_b/N_0$  performance of various coded modulation schemes having MAP decoding complexity associated with 128-trellis states, when communicating over uncorrelated Rayleigh channels using 8PSK modulation.

- [4] D. F. Yuan, P. Zhang, Q. Wang and W. E. Stark, "A Novel Multilevel Codes With 16QAM," *IEEE Wireless Communications and Networking Conference*, pp. 260–263, 2002.
- [5] F. Schreckenbach and G. Bauch, "EXIT charts for iteratively decoded multilevel modulation," *12th European Signal Processing Conference (EUSIPCO)*, 2004.
- [6] D. Divsalar, S. Dolinar and F. Pollara, "Serial Concatenated Trellis Coded Modulation with Rate-1 Inner Code," *IEEE Global Telecommunications Conference*, pp. 777–782, Nov. 2000.
- [7] M. Isaka and H. Imai, "On the Iterative Decoding of Multilevel Codes," *IEEE Journal on Selected Areas in Comms*, vol. 19, pp. 935–943, May 2001.
- [8] K. R. Narayanan, "Effect of Precoding on the Convergence of Turbo Equalization for Partial Response Channels," *IEEE Journal on Selected Areas in Communications*, pp. 686–698, Apr. 2001.
- [9] L. Hanzo, T. H. Liew and B. L. Yeap, *Turbo Coding, Turbo Equalisation and Space Time Coding for Transmission over Wireless channels*. New York, USA: John Wiley IEEE Press, 2002.